

# Turbulent Friction in Rough Pipes and the Energy Spectrum of the Phenomenological Theory

G. Gioia and Pinaki Chakraborty

*Department of Theoretical and Applied Mechanics, University of Illinois, Urbana, Illinois 61801, USA*  
(Received 12 May 2005; published 30 January 2006)

The classical experiments on turbulent friction in rough pipes were performed by Nikuradse in the 1930s. Seventy years later, they continue to defy theory. Here we model Nikuradse's experiments using the phenomenological theory of Kolmogórov, a theory that is widely thought to be applicable only to highly idealized flows. Our results include both the empirical scalings of Blasius and Strickler and are otherwise in minute qualitative agreement with the experiments; they suggest that the phenomenological theory may be relevant to other flows of practical interest; and they unveil the existence of close ties between two milestones of experimental and theoretical turbulence.

DOI: 10.1103/PhysRevLett.96.044502

PACS numbers: 47.27.nb, 47.27.Cn, 47.27.Jv

Turbulence is the unrest that spontaneously takes over a streamline flow adjacent to a wall or obstacle when the flow is made sufficiently fast. Although most of the flows that surround us in everyday life and in nature are turbulent flows over rough walls, these flows have remained among the least understood phenomena of classical physics [1,2]. Thus, one of the weightier experimental studies of turbulent flows on rough walls, and the most useful in common applications, is yet to be explained theoretically 70 years after its publication. In that study [3], Nikuradse elucidated how the friction coefficient between the wall of a pipe and the turbulent flow inside depends on the Reynolds number of the flow and the roughness of the wall. The friction coefficient,  $f$ , is a measure of the shear stress (or shear force per unit area) that the turbulent flow exerts on the wall of a pipe; it is customarily expressed in dimensionless form as  $f = \tau/\rho V^2$ , where  $\tau$  is the shear stress,  $\rho$  is the density of the liquid that flows in the pipe, and  $V$  is the mean velocity of the flow. The Reynolds number is defined as  $Re = VR/\nu$ , where  $R$  is the radius of the pipe and  $\nu$  the kinematic viscosity of the liquid. Last, the roughness is defined as the ratio  $r/R$  between the size  $r$  of the roughness elements (sand grains in the case of Nikuradse's experiments) that line the wall of the pipe and the radius of the pipe.

Nikuradse presented his data in the form of six curves, the log-log plots of  $f$  versus  $Re$  for six values of the roughness [3]. These curves are shown in Fig. 1. At the onset of turbulence [4], at a  $Re$  of about 3000, all six curves rise united in a single bundle. At a  $Re$  of about 3500, the bundle bends downward to form a marked *hump*, and then it plunges in accord with Blasius's empirical scaling [5],  $f \sim Re^{-1/4}$ , as one by one in order of decreasing roughness the curves start to careen away from the bundle. After leaving the bundle, which continues to plunge, each curve sets out to trace a *belly* [6] as it steers farther from the bundle with increasing  $Re$ , and then flexes towards a terminal, constant value of  $f$  that is in keeping with Strickler's empirical scaling [7],  $f \sim (r/R)^{1/3}$ . For 70 years

now, our understanding of these curves has been aided by little beyond a pictorial narrative of roughness elements being progressively exposed to the turbulent flow as  $Re$  increases [8].

In our theoretical work, we adopt the phenomenological imagery of "turbulent eddies" [9–11] and use the spectrum of turbulent energy [12] at a length scale  $\sigma$ ,  $E(\sigma)$ , to determine the velocity of the eddies of size  $s$ ,  $u_s$ , in the form  $u_s^2 = \int_0^s E(\sigma)\sigma^{-2}d\sigma$ , where  $E(\sigma) = A\varepsilon^{2/3}\sigma^{5/3}c_d(\eta/\sigma)c_e(\sigma/R)$ . Here  $A$  is a dimensionless constant,  $\varepsilon$  is the turbulent power per unit mass,  $\eta = \nu^{3/4}\varepsilon^{-1/4}$  is the viscous length scale,  $R$  is the largest length scale in the flow,  $A\varepsilon^{2/3}\sigma^{5/3}$  is the Kolmogórov spectrum (which is valid in the inertial range,  $\eta \ll \sigma \ll R$ ), and  $c_d$  and  $c_e$  are dimensionless corrections for the dissipative range and the energetic range, respectively. For  $c_d$  we adopt an exponential form,  $c_d(\eta/\sigma) = \exp(-\beta\eta/\sigma)$  (which gives  $c_d \approx 1$  except in the dissipative range, where  $\sigma \approx \eta$ ), and for  $c_e$  the form proposed by von Kármán,

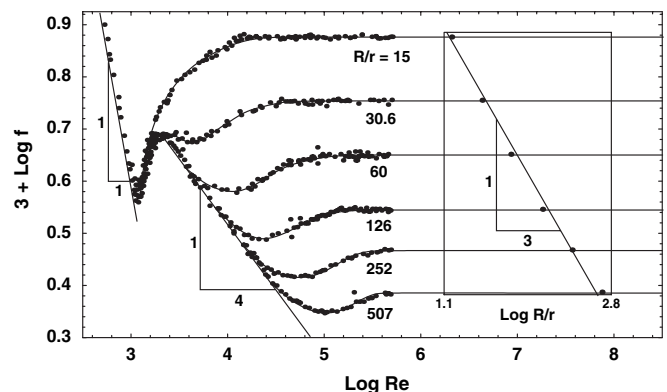


FIG. 1. Nikuradse's data. Up to a  $Re$  of about 3000 the flow is streamlined (free from turbulence) and  $f \sim 1/Re$ . Note that for very rough pipes (small  $R/r$ ) the curves do not form a belly at intermediate values of  $Re$ . Inset: verification of Strickler's empirical scaling for  $f$  at high  $Re$ ,  $f \sim (r/R)^{1/3}$ .

$c_e(\sigma/R) = [1 + \gamma(\sigma/R)^2]^{-17/6}$  (which gives  $c_e \approx 1$  except in the energetic range, where  $\sigma \approx R$ ), where  $\beta$  and  $\gamma$  are dimensionless constants [12]. To obtain expressions for  $u_s$  and  $\eta$  in terms of  $Re$ ,  $r/R$ , and  $V$ , we invoke the usual scalings [13],  $\varepsilon = \kappa_\varepsilon u_R^3/R$  (Taylor's scaling [14], where  $u_R$  is the characteristic velocity of the largest eddies and  $\kappa_\varepsilon$  a dimensionless constant) and  $u_R = \kappa_u V$  (where  $\kappa_u$  is a dimensionless constant). Then, we can write  $\eta = bRRe^{-3/4}$ , where  $b \equiv (\kappa_\varepsilon \kappa_u^3)^{-1/4}$ , and (after changing the integration variable to  $x \equiv \sigma/R$ )  $u_s^2 = A\kappa_\varepsilon^{2/3} u_R^2 \int_0^{s/R} x^{-1/3} c_d(bRe^{-3/4}/x) c_e(x) dx$ . For  $s \ll R$  we can set  $c_e = 1$ , compute the integral, and let  $Re \rightarrow \infty$  to obtain  $u_s^2 = (3/2)A\kappa_\varepsilon^{2/3} u_R^2 (s/R)^{2/3}$ , or  $u_s^2 \sim u_R^2 (s/R)^{2/3}$ , a well-known result of the phenomenological theory. Further, for consistency with Taylor's scaling we must have  $A\kappa_\varepsilon^{2/3} = 2/3$  (so that  $u_s = u_R$  for  $s = R$ ) and therefore  $u_s^2 = \kappa_u^2 V^2 (2/3) \int_0^{s/R} x^{-1/3} c_d(bRe^{-3/4}/x) c_e(x) dx$ .

We now seek to derive an expression for  $\tau$ , the shear stress on the wall of the pipe. We assume a viscous layer of constant thickness  $a\eta$ , where  $a$  is a dimensionless constant, and call  $W$  a wetted surface parallel to the peaks of the viscous layer (Fig. 2). Then,  $\tau$  is effected by momentum transfer across  $W$ . Above  $W$ , the velocity of the flow scales with  $V$ , and the fluid carries a high horizontal momentum per unit volume ( $\sim \rho V$ ). Below  $W$ , the velocity of the flow is negligible, and the fluid carries a negligible horizontal momentum per unit volume. Now consider an eddy that straddles the wetted surface  $W$ . This eddy transfers fluid of high horizontal momentum downwards across  $W$  and fluid of negligible horizontal momentum upwards across  $W$ . The net rate of transfer of momentum across  $W$  is set by the velocity normal to  $W$ , which velocity is provided by the eddy. Therefore, if  $v_n$  denotes the velocity normal to  $W$  provided by the *dominant* eddy that straddles  $W$ , then the shear stress effected by momentum transfer across  $W$  scales in the form  $\tau \sim \rho V v_n$ .

In order to identify the dominant eddy that straddles  $W$ , let us denote by  $s = r + a\eta$  the size of the largest eddy that fits the coves between successive roughness elements. Eddies much larger than  $s$  can provide only a negligible

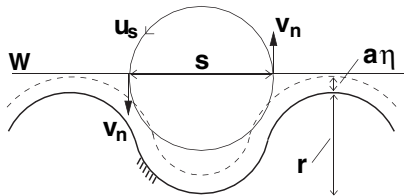


FIG. 2. Schematic of the immediate vicinity of the wall with roughness elements of size  $r$  covered by a viscous layer of uniform thickness  $a\eta$ . The distance between roughness elements is about equal to the height of the roughness elements, as in Nikuradse's experiments [20]. The horizontal line is the trace of a wetted surface  $W$  tangent to the peaks of the viscous layer.

velocity normal to  $W$ . (This observation is purely a matter of geometry.) On the other hand, eddies smaller than  $s$  can provide a sizable velocity normal to  $W$ . Nevertheless, if these eddies are much smaller than  $s$ , their velocities are overshadowed by the velocity of the eddy of size  $s$ . Thus,  $v_n$  scales with  $u_s$ , which is the velocity of the eddy of size  $s$ , and the dominant eddy is the largest eddy that fits the coves between successive roughness elements. We conclude that  $\tau \sim \rho V u_s$ , or  $\tau = \kappa_\tau \rho V u_s$  (where  $\kappa_\tau$  is a dimensionless constant of order 1), and therefore  $f = \kappa_\tau u_s / V$  or

$$f = K \left( \int_0^{s/R} x^{-1/3} c_d(bRe^{-3/4}/x) c_e(x) dx \right)^{1/2}, \quad (1)$$

where  $K \equiv \kappa_\tau \kappa_u \sqrt{2/3}$ ,  $s/R = r/R + abRe^{-3/4}$ , and  $b \equiv (\kappa_\varepsilon \kappa_u^3)^{-1/4}$ . Equation (1) gives  $f$  as an explicit function of the Reynolds number  $Re$  and the roughness  $r/R$ .

To evaluate computationally the integral of (1), we set  $\beta = 2.1$ ,  $\gamma = 6.783$  (the values given in [12]),  $a = 5$  ( $5\eta$  being a common estimation of the thickness of the viscous layer),  $\kappa_\varepsilon = 5/4$  (a value that follows from Kolmogórov's four-fifths law [15]),  $\kappa_u = 0.036$  ( $0.036 \pm 0.005$  being the value measured in pipe flow by Antonia and Pearson [16]),  $b \equiv (\kappa_\varepsilon \kappa_u^3)^{-1/4} = 11.4$ , and treat  $\kappa_\tau$  as a free parameter (albeit a parameter constrained by theory to be of order 1). With  $\kappa_\tau = 0.5$  (and therefore  $K = 0.015$ ), Eq. (1) gives the plots of Fig. 3. (Note that a different value of  $\kappa_\tau$  would give the same plots except for a vertical translation.) These plots show that (1) is in excellent qualitative agreement with Nikuradse's data, right from the onset of turbulence, including the hump and, for relatively low roughness, the bellies. These plots remain qualitatively the same even if the value of any of the parameters is changed widely. In

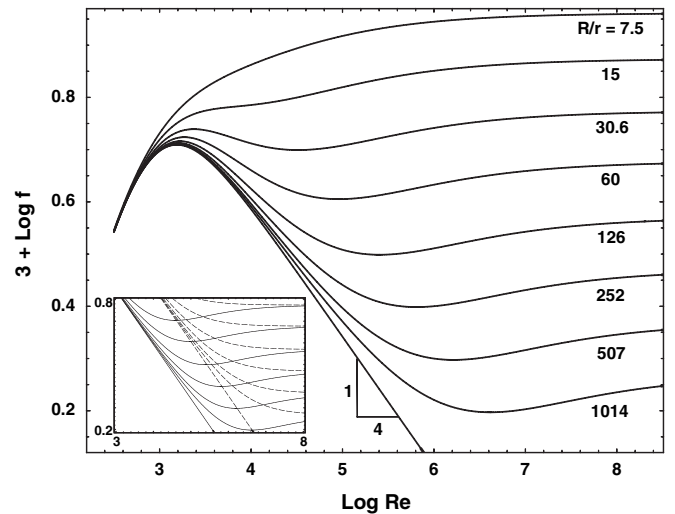


FIG. 3. Plot of (1). Inset: Plot of (2) (no correction for the energetic range: solid lines) and plot of (2) with  $\gamma = 0$  (no correction for the energetic range and the dissipative range: dashed lines).

particular, there is always a hump, and there are always bellies: these are robust features closely connected with the overall form of the spectrum of turbulent energy. The connections will become apparent after the discussion that follows.

To help interpret our results, we compute  $f$  without including the correction for the energetic range—that is, setting  $\gamma = 0$ . In this case, the integral of (1) may be evaluated analytically, with the result

$$f = K(r/R + ab \text{Re}^{-3/4})^{1/3} \sqrt{F(y)}, \quad (2)$$

where  $F(y) = y^{2/3} \Gamma_{-2/3}(y)$ ,  $\Gamma_{-2/3}$  is the gamma function of order  $-2/3$ , and  $y = \beta \eta / s = \beta b \text{Re}^{-3/4} (r/R + ab \text{Re}^{-3/4})^{-1}$ . With the same values of  $\kappa_\tau$ ,  $\kappa_u$ ,  $a$ ,  $b$ , and  $\beta$  as before, Eq. (2) gives the solid-line plots in the inset of Fig. 3. The hump is no more. We conclude that the hump relates to the energetic range. Further, with the exception of the hump at relatively low  $\text{Re}$ , the plots of (1) coincide with the plots of (2); thus, we can study (2) to reach conclusions about (1) at intermediate and high  $\text{Re}$ . For example, Eq. (2) gives  $f \sim (r/R)^{1/3}$  for  $r \gg a\eta$  and  $f \sim \text{Re}^{-1/4}$  for  $r \ll a\eta$ . It follows that both (2) and (1) give a gradual transition between the empirical scalings of Blasius and Strickler [17], in accord with Nikuradse's data.

If we set  $\beta = 0$  in addition to  $\gamma = 0$  (that is, if we exclude the correction for the dissipative range in addition to the correction for the energetic range), Eq. (2) simplifies to  $f = \kappa_\tau \kappa_u (r/R + ab \text{Re}^{-3/4})^{1/3}$ . With the same values of  $\kappa_\tau$ ,  $\kappa_u$ ,  $a$ , and  $b$  as before, this expression gives the dashed-line plots in the inset of Fig. 3. Now the bellies are no more. We conclude that the bellies relate to the dissipative range. The dissipation depresses the values of  $f$  at relatively low and intermediate  $\text{Re}$ , leading to the formation of the bellies of Nikuradse's data.

We are ready to explain the unfolding of Nikuradse's data in terms of the varying habits of momentum transfer with increasing  $\text{Re}$  (Fig. 4). At relatively low  $\text{Re}$ , the inertial range is immature, and the momentum transfer is dominated by eddies in the energetic range, whose velocity scales with  $V$ , and therefore with  $\text{Re}$ . Consequently, an

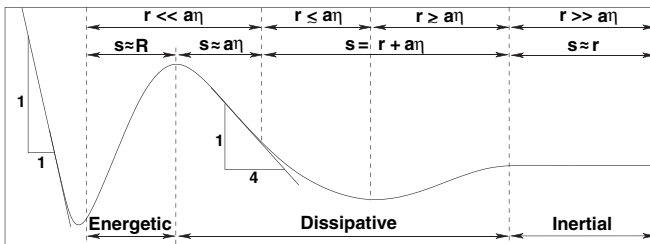


FIG. 4. Schematic of the relations among a generic Nikuradse curve, the spectrum of turbulent energy, the size of the roughness elements, the thickness of the viscous layer, and the size of the dominant eddies.

increase in  $\text{Re}$  leads to a more vigorous momentum transfer—and to an increase in  $f$ . This effect explains the rising part of the hump. At higher  $\text{Re}$ , the momentum transfer is dominated by eddies of size  $s \approx a\eta \gg r$ . Since  $\eta \sim \text{Re}^{-3/4}$ , with increasing  $\text{Re}$  the momentum transfer is effected by ever smaller (and slower) eddies, and  $f$  lessens as  $\text{Re}$  continues to increase. This effect explains the plunging part of the hump—the part governed by Blasius's scaling. At intermediate  $\text{Re}$ ,  $s = r + a\eta$  with  $r \approx a\eta$ . Because of the decrease in  $\eta$ ,  $s$  continues to lessen as  $\text{Re}$  continues to increase, but at a lower rate than before, when it was  $s \approx a\eta \gg r$ . Thus, the curve associated with  $r$  deviates from Blasius's scaling and starts to trace a belly. As  $\eta$  continues to decrease, the dominant eddies become decidedly larger than the smaller eddies in the inertial range, which is well established now, and any lingering dissipation at length scales larger than  $s$  must cease. This effect explains the rising part of the belly. Last, at high  $\text{Re}$ ,  $s \approx r \gg a\eta$ . As  $\text{Re}$  increases further,  $\eta$  lessens and new, smaller eddies populate the flow and become jumbled with the preexisting eddies. Yet the momentum transfer continues to be dominated by eddies of size  $r$ , and  $f$  remains invariant. This effect explains Nikuradse's data at high  $\text{Re}$ , where  $f$  is governed by Strickler's scaling.

We have predicated Eq. (1) on the assumption that the turbulent eddies are governed by the phenomenological theory of turbulence. The theory was originally derived for isotropic and homogeneous flows, but recent research [18] suggests that it applies to much more general flows as well. Our results indicate that even where the flow is anisotropic and inhomogeneous—as is the case in the vicinity of a wall—the theory gives an approximate solution that embodies the essential structure of the complete solution (including the correct scalings of Blasius and Strickler) and is in detailed qualitative agreement with the observed phenomenology. Remarkably, the qualitative agreement holds starting at the very onset of turbulence, in accord with experimental evidence that “in pipes, turbulence sets in suddenly and fully, without intermediate states and without a clear stability boundary” [4]. The deficiencies in quantitative agreement point to a need for corrections to account for the effect of the roughness elements on the dissipative range as well as for the effect of the overall geometry on the energetic range.

In conclusion, to a good approximation the eddies in a pipe are governed by the spectrum of turbulent energy of the phenomenological theory. The size of the eddies that dominate the momentum transfer close to the wall is set by a combination of the size of the roughness elements and the viscous length scale. As a result, the dependence of the turbulent friction on the roughness and the Reynolds number is a direct manifestation of the distribution of turbulent energy given by the phenomenological theory. This close relation between the turbulent friction and the phenomenological theory [19] may be summarized in the follow-

ing observation: the similarity exponents of Blasius and Strickler are but recast forms of the exponent  $5/3$  of the Kolmogórov spectrum.

We are thankful to F. A. Bombardelli, N. Goldenfeld, and W. R. C. Phillips for a number of illuminating discussions. J. W. Phillips kindly read our manuscript and made suggestions for its improvement.

- 
- [1] J. Jiménez, *Annu. Rev. Fluid Mech.* **36**, 173 (2004).
- [2] M. R. Raupach, R. A. Antonia, and S. Rajagopalan, *Appl. Mech. Rev.* **44**, 1 (1991).
- [3] Reprinted in English in J. Nikuradse, NACA Tech. Memo. **1292** (1950).
- [4] B. Hof *et al.*, *Science* **305**, 1594 (2004).
- [5] L. Prandtl, *Essentials of Fluid Dynamics* (Blackie & Son, London, 1953), 3rd ed., Chap. III.11.
- [6] In Nikuradse's experiments the average distance between roughness elements was about the same as the height of the roughness elements,  $r$ . This is the type of single-length-scale roughness that concerns us here. For this type of roughness, there are always bellies in the log-log plots of  $f$  vs  $Re$ . [For similar results on open channels, see Warwick's data in, e.g., O. Kirshmer, *Rev. Gen. Hydraulique* **51**, 115 (1949), in French.] For more complicated types of roughness, where roughness elements of many different sizes are present (as is commonly the case in commercial pipes), the bellies may be absent (see, e.g., the paper by Kirshmer cited above) or perhaps present after all [see, e.g., C. F. Colebrook and C. M. White, *Proc. R. Soc. A* **161**, 367 (1937)]. For the latest experimental data and discussion of this issue, see J. J. Allen, M. A. Shockling, and A. J. Smits, *Phys. Fluids* **17**, 121702 (2005), and M. A. Shockling, MSE dissertation, Princeton University, 2005.
- [7] Reprinted in English in A. Strickler, *Contribution to the Question of a Velocity Formula and Roughness Data for Streams, Channels and Close Pipelines*, translation by T. Roesgen and W. R. Brownlie (Caltech, Pasadena, 1981). The value  $1/3$  of the exponent of  $r/R$  in Strickler's scaling can be derived by dimensional analysis from the value  $2/3$  of the exponent of the hydraulic radius in Manning's empirical formula for the average velocity of the flow in a rough open channel. Manning obtained his formula independently of Strickler, on the basis of different experimental data.
- [8] See, e.g., V. T. Chow, *Open-Channel Hydraulics* (McGraw-Hill, New York, 1988).
- [9] L. F. Richardson, *Proc. R. Soc. A* **110**, 709 (1926).
- [10] Reprinted in English in A. N. Kolmogórov, *Proc. R. Soc. A* **434**, 9 (1991).
- [11] U. Frisch, *Turbulence* (Cambridge University Press, Cambridge, 1995).
- [12] S. B. Pope, *Turbulent Flows* (Cambridge University Press, Cambridge, 2000).
- [13] See, e.g., H. Tennekes and J. L. Lumley, *A First Course in Turbulence* (MIT Press, Cambridge, MA, 1972).
- [14] G. I. Taylor, *Proc. R. Soc. A* **151**, 421 (1935); D. Lohse, *Phys. Rev. Lett.* **73**, 3223 (1994). The existence of an upper bound on  $\varepsilon$  that is independent of the viscosity has been proved *mathematically*; see Ch. R. Doering and P. Constantin, *Phys. Rev. Lett.* **69**, 1648 (1992).
- [15] Kolmogórov's four-fifths law reads  $\bar{u}_r^3 = -(4/5)\varepsilon r$ , where the left-hand side is the third-order structure function. Substituting  $r = R$  and estimating  $|\bar{u}_r^3| = u_R^3$  leads to  $\varepsilon = (5/4)u_R^3/R$ , or  $\kappa_\varepsilon = 5/4$ . Experimental estimates of  $\kappa_\varepsilon$  are  $O(1)$ ; see K. R. Sreenivasan, *Phys. Fluids* **10**, 528 (1998).
- [16] R. A. Antonia and B. R. Pearson, *Flow, Turbul. Combust.* **64**, 95 (2000). For comparison, Tennekes and Lumley give  $\kappa_u = 0.033$  for the atmosphere's turbulent boundary layer [13].
- [17] G. Gioia and F. A. Bombardelli, *Phys. Rev. Lett.* **88**, 014501 (2002).
- [18] B. Knight and L. Sirovich, *Phys. Rev. Lett.* **65**, 1356 (1990); T. S. Lundgren, *Phys. Fluids* **14**, 638 (2002); T. S. Lundgren, *ibid.* **15**, 1074 (2003). Yet the view of anisotropy as a perturbation superposed on the isotropic flow (see, e.g., L. Biferale and I. Procaccia, nlin.CD/0404014) might break down close to a wall, where the exponents themselves might change [see M. Casciola, P. Gualtieri, B. Jacob, and R. Piva, *Phys. Rev. Lett.* **95**, 024503 (2005)]. Nevertheless, note (i) that the exponent of the second-order structure function appears to change only by a little and (ii) that the Kolmogórov exponent does give the exact scalings of Blasius and Strickler, whereas any modified exponent would not.
- [19] The close connection between the turbulent friction and the phenomenological spectrum suggests that in turbulence, just as in phase transitions, large-scale phenomena are direct manifestations of the small-scale statistics. The parallel with phase transitions has been adduced by Goldenfeld, who was prompted by our results to reanalyze Nikuradse's data and conclude that (2) is consistent with a turbulent analogue of Widom scaling near critical points. See N. Goldenfeld, following Letter, *Phys. Rev. Lett.* **96**, 044503 (2006).
- [20] Our schematic of Fig. 2 may seem to resemble the "d-type roughness" of A. E. Perry, W. H. Schofield, and P. N. Joubert, *J. Fluid Mech.* **37**, 383 (1969). According to these authors, for this type of roughness the turbulent friction does not asymptotically approach a constant value at high  $Re$ . Nevertheless, as pointed out by Jiménez [1], the distinction between  $k$ -type roughness (including the type of roughness in Nikuradse's pipes) and  $d$ -type roughness appears to have been predicated on limited experimental data, and must be regarded with caution. In any case, the schematic of Fig. 2 represents the rough walls of Nikuradse's experiments [6] and does lead to predictions that are in accord with those experiments.